Eur. J. Mech. B/Fluids, **17,** n° 6, 823-846, 1998

Experiments on localized disturbances in a flat plate boundary layer. Part 1. The receptivity and evolution of a localized free stream disturbance

K. J. A. WESTIN ([1]) *, A. A. BAKCHINOV ([1]), ([2]) **,
V. V. KOZLOV ([2]) and P. H. ALFREDSSON ([1])

ABSTRACT. – The receptivity of a laminar boundary layer to free stream disturbances has been experimentally investigated through the introduction of deterministic localized disturbances upstream of a flat plate mounted in a wind tunnel. Hot-wire measurements indicate that the spanwise gradient of the normal velocity component (and hence the streamwise vorticity) plays an essential role in the transfer of disturbance energy into the boundary layer. Inside the laminar boundary layer the disturbances were found to give rise to the formation of longitudinal structures of alternating high and low streamwise velocity. Similar streaky structures exist in laminar boundary layers exposed to free stream turbulence, in which the disturbance amplitude increases in linear proportion to the displacement thickness. In the present study the perturbation amplitude of the streaks was always decaying for the initial amplitudes used, in contrast to the growing fluctuations that are observed in the presence of free stream turbulence. This points out the importance of the continuous influence from the free stream turbulence along the boundary layer edge. © Elsevier, Paris.

Keywords: Boundary-layer, streaky-structures, transition.

1. Introduction

Transition from laminar to turbulent flow in wall bounded shear flows follows a sequence which can be divided into excitation of perturbations, amplification of induced disturbances and finally breakdown to turbulence. Numerous experimental investigations have demonstrated that the transition process strongly depends on the ambient disturbance level. As early as 1883 Reynolds suggested that transition in pipe flow shifts upstream with increasing disturbance intensity in the incoming flow. It is recognized that various types of external disturbances play an important role in the transition process, for example natural free stream turbulence, acoustic perturbations, vibrations, surface roughnesses, etc. (*see*, for instance, Morkovin and Reshotko, 1990; Kozlov and Ryzhov, 1990 and Westin *et al.*, 1994). Furthermore, the development of the disturbances inside the boundary layer depends not only on the source of generation, but also on its intensity as well as its spectral composition. The mechanisms through which disturbances are introduced into a boundary layer are usually denoted as receptivity mechanisms, and at present the knowledge about receptivity lags behind many other areas of transition research. Since a full description of the transition process requires that the initial conditions are known, the understanding of the receptivity process is crucial for the development of useful and reliable prediction methods.

A majority of earlier receptivity studies has focussed on the generation of Tollmien-Schlichting (TS) waves due to acoustical disturbances (*see* Nishioka and Morkovin, 1986 for a review). In order to efficiently induce

* Presently at Vattenfall Utveckling AB, S-81426 Älvkarleby, Sweden.
** Presently at Chalmers University of Technology, Thermo- and Fluid Dynamics, S-412 96 Göteborg, Sweden.
([1]) Dept. Mechanics, Royal Institute of Technology, S-10044 Stockholm, Sweden.
([2]) Institute of Theoretical and Applied Mechanics, Russian Academy of Sciences, Siberian Branch, 630090 Novosibirsk, Russia.

0997-7546/98/06/© Elsevier, Paris

TS-waves with sound the acoustical perturbations have to interact with local changes in the mean flow, for instance in the leading edge region or close to surface roughnesses. Another source of disturbance is free stream turbulence (FST). It has been observed that FST can induce at least two types of boundary layer disturbances: randomly occurring TS-wave packets, and large amplitude low-frequency fluctuations in the streamwise velocity component. Unless the FST-level Tu is low, the latter type of disturbances will be dominant inside the boundary layer with rms-amplitudes in the streamwise velocity component of the order of 10% before transition occurs (Tu is defined as $u_{rms,0}/U_0$ measured at the leading edge, where $u_{rms,0}$ is the streamwise component of the free stream turbulence and U_0 is the free stream velocity). However, both types of disturbances may co-exist in the boundary layer, even at rather high levels of FST, and interaction between them may be of importance for transition.

1.1. Some notes on receptivity to free stream disturbances

The influence from free stream turbulence on the transition process is well-known both from scientific experiments and technical applications. Extensive measurements of the effects of relatively low levels of free stream turbulence ($Tu < 0.3\%$) have been undertaken by Kendall (1985, 1990, 1991, 1993). These studies were mainly focussed on the possible generation of TS-wave packets due to the free stream turbulence, using a sophisticated measurement technique in which the signals from a large number of wall-mounted microphones were correlated. The results showed an increased generation of TS-wave packets with increasing Tu, and the change in amplitude was larger than the change in FST-level. Furthermore, the growth rates of the wave packets were larger than predicted by linear theory, an observation which was interpreted as a result of distributed forcing along the boundary layer edge. Kendall also showed that the bluntness of the leading edge influenced the TS-wave generation, with a stronger generation in the case of a blunt nose.

The important role of the leading edge was also demonstrated in the experimental study by Kachanov *et al.*, (1978). In that case a two-dimensional (2D), periodic free stream perturbation was generated by means of a vibrating ribbon positioned upstream of the flat plate leading edge. The ribbon generates fluctuations in the wall-normal direction which affect a significant region of the flow. The wall-normal fluctuations generated a localized region of disturbed flow located directly at the leading edge, which acted as a source of generation for TS-waves in the boundary layer. This localized region appeared whether the ribbon was positioned below or above the stagnation streamline.

Dovgal *et al.*, (1980) demonstrated the possibility to generate 2D TS-waves by a vibrating ribbon mounted in the free stream at a supercritical Reynolds number. In this case there was no influence from the leading edge. The experiment clearly indicated the possibility to excite TS-waves through the interaction of external, non-vortical fluctuations with the boundary layer. It means that TS-waves can be generated not only close to the leading edge of the model, but also under conditions with strong spatially non-uniform external perturbations.

Besides the increased generation of TS-wave packets, Kendall (1985) observed a different type of disturbances which he denoted as the Klebanoff-mode (Klebanoff, 1971). This is characterized by low-frequency fluctuations, mainly caused by irregular motion of long structures with narrow spanwise scales inside the boundary layer. The amplitude maximum is found approximately in the middle of the boundary layer, and the amplitude is growing downstream in linear proportion to the displacement thickness. Similar observations were made in the study by Westin *et al.*, (1994) at a slightly higher FST-level ($Tu = 1.5\%$). The formation of long and narrow streaky structures has also been observed in flow visualisations by Kendall (1985), Gulyaev *et al.*, (1989) and recently by Alfredsson and Matsubara (1996). In the paper by Morkovin and Reshotko (1990), two possibilities are suggested concerning the generation of these low-frequency fluctuations in the boundary layer: the generation due to direct action of streamwise vorticity in the FST, or, which was judged to be a more important mechanism,

the generation due to 'coherent vortex elements which extend from below to above the flat plate and thus get caught and strained by the leading edge'. In a recent experimental work by Watmuff (1997) almost immeasurable free-stream non-uniformities generated by the wind tunnel screens were found to result in the appearance of vortices at the leading edge, which gave rise to the Klebanoff modes in the boundary layer.

A complicating circumstance when studying transition at high levels of FST is the random character of the introduced disturbances, which are usually generated by grids positioned in the wind-tunnel. The study of details in the receptivity process close to the leading edge becomes an intricate task, which has to rely on the information that can be extracted from different correlation measurements. Similar difficulties is associated with the later stages of the transition process. Since the amplitudes of the described low-frequency fluctuations are usually quite large, many details in the transition process, such as different types of interactions or secondary instabilities, become difficult to detect. Consequently, there is a demand for more controllable disturbances which can be used in model experiments.

In a theoretical work by Goldstein *et al.,* (1992) it was found that a small vortical perturbation introduced ahead of a flat plate gave rise to small amplitude, non-linear spanwise motion in the boundary layer far downstream from the leading edge. An attempt to study the boundary layer response to a controlled free stream vortex has recently been presented by Bertolotti and Kendall (1997), who excited a stationary wing-tip vortex upstream of the leading edge of a flat plate. The vortex forced a streamwise velocity perturbation inside the growing boundary layer, and the disturbance amplitude increased linearly with the streamwise coordinate. The measurements were compared with computations by Bertolotti (*see* also Bertolotti, 1997), who considered the Parabolized Stability Equations (PSE) together with a free stream vortex model.

1.2. Some notes on localized disturbances in boundary layer flows

If a small amplitude disturbance is introduced at supercritical Reynolds numbers it usually results in a TS-wave packet. This was first studied by Gaster and Grant (1975), who observed a downstream development with phase speeds in agreement with TS-waves and a spanwise spreading of the wave packet. Further downstream, low-frequency oblique waves could be observed in the spectra, suggesting that subharmonic resonances were at play. Similar observations were made in experiments by Cohen *et al.,* (1991), who followed the evolution of the initially linear wave packet through the non-linear stage until it evolved into a turbulent spot. They also showed that for measurements in the region with subharmonic growth, the spanwise wave pattern was rather different whether the probe was positioned outside or inside the boundary layer. The distortion of the wave fronts observed inside the boundary layer was ascribed to an increased contribution from normal vorticity, which can be forced by growing three-dimensional subharmonic waves (*see* also section 1.3).

A much stronger initial amplitude was used by Amini and Lespinard (1982), who obtained a structure which they denoted as an 'incipient spot'. The propagation velocities of the front and rear part were $0.95U_0$ and $0.5U_0$ respectively, and it showed a rather slow spanwise spreading with a lateral growth angle of about $4°$.

Grek *et al.,* (1985, 1991b) showed that three different types of disturbances could be obtained from a point source positioned inside a flat plate boundary layer. Beside the wave packet and the turbulent spot, they found a third type of disturbance. The spanwise spreading of this structure was very small throughout its evolution (in contrast to TS-wave packets), and the propagation speed for the front part of the disturbance was around 80% of the free stream velocity. Furthermore, the maximum disturbance amplitude was found approximately in the middle of the boundary layer, but with a downstream decay of the amplitude. Due to the limited connection with the wall and the large propagation speed, this type of boundary layer disturbance was at the time named a 'Puff'. This term was borrowed from Wygnanski *et al.,* (1975), who used it to denote a localized disturbance in pipe flow.

A similar 'puff-like' structure was also observed by Breuer and Haritonidis (1990). This transient part propagated with the local mean velocity, it was stretched in the streamwise direction but showed only a very limited spanwise spreading. However, the disturbance amplitude of the transient decayed quickly, and the disturbance became dominated by a growing TS-wave packet.

The previously discussed localized disturbances were all generated with the disturbance source positioned inside the boundary layer, although the methods varied slightly (movable membrane, injection through hole or injection through a perforated plate). Consequently, the studies do not give any information concerning the receptivity to free stream disturbances. An attempt to generate localized disturbances from the free stream was carried out by Grek *et al.,* (1991a), who introduced a short duration jet through a pipe located upstream of the leading edge. This resulted in boundary layer disturbances with characteristics similar to the previously described 'puff'.

1.3. Transient growth

There are many observations showing that longitudinal streaky structures are present in so-called 'by-pass' transition in different types of shear-flows. The streak formation is a result which is supported by theoretical studies on algebraic or transient growth. These studies have shown that transient growth, which is governed by linearized equations, can in many cases exhibit much larger energy growth over short times than any exponentially growing eigenmode (*see* Henningson, 1995 for a review). Butler and Farrell (1992) studied optimal disturbances in a Blasius boundary layer (under the parallel flow assumption) and found that disturbances resembling streamwise vortices give the largest energy growth over short times. Although the streamwise vortex itself is continuously damped, it generates large disturbance amplitudes in the u-component. The basic idea is that a wall-normal displacement of a fluid element in a shear layer will cause a perturbation in the streamwise velocity component, since the fluid element will initially retain its horizontal momentum. This effect is often referred to as *lift-up* (Landahl, 1977, 1980). Within the inviscid approximation the streamwise perturbation velocity (u) will grow algebraically in time. If viscosity is taken into account, the disturbance will eventually start to decay after a region with transient growth.

An important condition for the occurrence of strong transient (or algebraic) growth is the existence of three-dimensional disturbances. This can be understood by considering the linearized, inviscid equation for the normal vorticity ($\eta = \partial u/\partial z - \partial w/\partial x$):

$$\left(\frac{\partial}{\partial t} + U\frac{\partial}{\partial x}\right)\eta = -U'\frac{\partial v}{\partial z}$$

where u, v and w are the perturbation velocity components in the streamwise (x), wall-normal (y) and spanwise (z) directions respectively, whereas U is the streamwise mean velocity component. U' denotes the derivative $\partial U/\partial y$.

The forcing term in the right hand side depends on the spanwise gradients of the wall-normal perturbation velocity. Consequently, a 3D disturbance with strong streamwise vorticity can together with a shear layer force a growth in the normal vorticity. Since the disturbance is elongated in the streamwise direction due to the mean shear, this will be observed as streaks with high and low streamwise perturbation velocity.

It should be emphasized that the majority of theoretical works on algebraic growth deals with the temporal stability of parallel flows. In a recent study by Luchini (1996) the spatial growth of 3D perturbations in the Blasius boundary layer was considered. In the framework of Prandtl's boundary layer approximation a Reynolds-number-independent algebraic growth was observed for some 3D modes. The viscous dissipation in

the expanding boundary layer was not sufficient to compensate for the algebraic growth, thus leading to an unbounded growth of the streamwise perturbation velocity.

Since the rapid transition to turbulence in a boundary layer subjected to a high level of free stream turbulence is affected by the existence of this kind of longitudinal disturbances, the understanding of their role in the transition process is of great importance. The present study is a continuation of a series of experiments on the effects of free stream turbulence in the transition process (Westin *et al.*, 1994; Boiko *et al.*,1994). The aim is to generate a controlled free stream disturbance which can serve as a model for free stream vortices impinging onto the boundary layer in the case of moderate and high levels of FST. Some preliminary results from the present experiment was also reported in Bakchinov *et al.*, (1995). The study makes use of a similar technique to introduce disturbances into the free stream as was used by Grek *et al.*, (1991), and the experimental set-up and measurement technique are further described in section 2. The results are discussed in section 3, where much attention is focussed on the disturbance characteristics in the vicinity of the leading edge. Comparisons with laminar boundary layers subjected to free stream turbulence are also shown, in order to elucidate similarities as well as differences between the induced disturbances. In section 4 the results are discussed together with results from other experimental, theoretical and numerical studies, and, finally, section 5 summarizes the most important observations.

2. Experimental set-up and measurement technique

The experiments were carried out in the closed-loop MTL (Minimum Turbulence Level) wind tunnel at KTH, Stockholm. The background turbulence intensity (streamwise fluctuations) with empty test section is approximately 0.02% of the free stream velocity (U_0). U_0 was in the range 6 to 8 m/s in the present experiment. The general outline of the experimental set-up is shown in Figure 1.

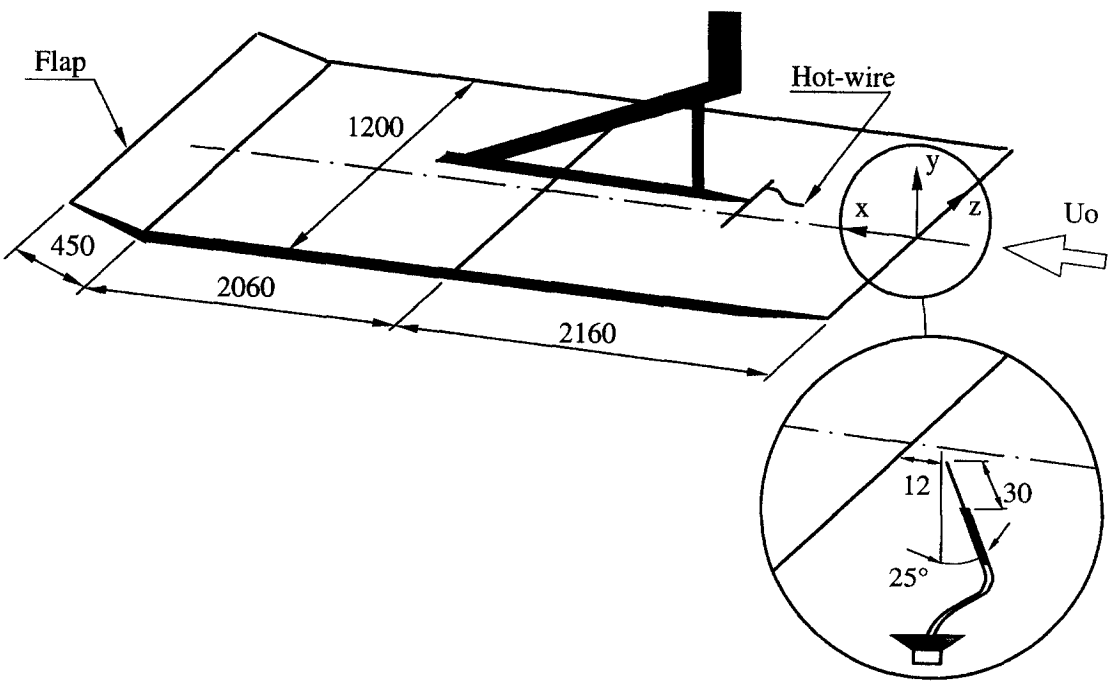

Fig. 1. – Outline of experimental set-up. Dimensions in mm.

A rectangular 1.2×4.22 m^2 flat plate was mounted horizontally in the 7 m long test section of 0.8×1.2 m^2 cross section, which was preceded by a contraction with ratio 9:1. The flat plate configuration was identical to the so-called set-up II described in Westin *et al.*, (1994), except for the traversing mechanism which was slightly modified. The ceiling and the floor of the test section were adjusted for a zero streamwise pressure gradient along the plate, and the stagnation line at the leading edge was controlled with a trailing edge flap. An asymmetric leading edge was used in order to minimize the region with non-zero pressure gradient close to the leading edge (for further details about the leading edge, we refer to Klingmann *et al.*, 1993).

The streamwise and normal velocity components were measured with constant-temperature hot wire anemometers, using both single and X-wire probes. The single wire probe was made of 2.5 μm platinum wire with a sensing length of 0.5 mm, and operated at a resistive overheat of 60 %. The probe was calibrated with a Prandtl tube in the free stream. A calibration function of the form

$$U = k_1(E^2 - E_0^2)^{1/n} + k_2(E - E_0)^{1/2}$$

was used, in which E is the anemometer output voltage at the velocity U, E_0 is the voltage at zero velocity, and k_1, k_2 and n are constants to be determined for the best fit to the calibration data. An X-wire probe was used for free stream measurements of streamwise and normal velocity components in the vicinity of the leading edge. It was made of 2.5 μm wires and had a cubic measurement volume smaller than 0.5 mm in side length. The probe was calibrated at several angles and flow velocities, from which a voltage pair (E_1, E_2) was obtained at each calibration point. Two third degree polynomial surfaces were fitted to the data, giving both u and v as functions of (E_1, E_2).

The data was acquired using a MacADIOS-adio A/D converter connected to a Macintosh computer, and another computer was used to control the servo motors for positioning of the probes. A right-handed co-ordinate system was used with x, y and z as the downstream, normal (to the plate surface) and spanwise directions respectively, with the origin on the centreline of the leading edge.

2.1. Generation of localized free stream disturbances

A vortical perturbation was generated in the free stream by introducing a short duration jet through a pipe mounted in the vicinity of the plate nose, as shown in Figure 1. The pipe had outer and inner diameters of 1.2 and 1.0 mm respectively, and was positioned 12 mm upstream of the leading edge and below the stagnation streamline. The pipe was slightly inclined in the streamwise direction, forming an angle of 25° with the normal to the wall.

A disturbance was produced by a loudspeaker located below the test section and connected to the pipe with a flexible tube. The loudspeaker was driven from the amplified output of a function generator, which provided the possibility to control the pulse duration time as well as the time between each individual pulse. The pulse time was chosen to 10 μs, and the number of pulses per second was typically 6. Every second pulse was positive, *i.e.* it caused an up-down-motion of the membrane, resulting in injection of fluid through the pipe. Consequently, the negative pulses caused a suction through the pipe, which, as expected, gave a much weaker free stream disturbance than the jet. The response time of the loudspeaker and pipe configuration was approximately 5 ms.

Most of the measurements were carried out by injection of air through the pipe and with a free stream velocity of 6.6 m/s. For this disturbance the end of the pipe was below the stagnation streamline and no effect of the wake behind the pipe could be detected in the undisturbed boundary layer. Some measurements were carried out by impulsive withdrawal of fluid through the pipe. In that case the end of the pipe was located closer to the stagnation streamline, and a small effect of its presence could be detected in the boundary layer. The data collection was triggered by the signal to the loud speaker, and in order to reduce the influence from

noise and stochastic disturbances, ensemble averaging of approximately 50 realizations was carried out at each spatial measurement point.

2.2. Data processing and presentation

In the paper the shape of the perturbations is presented as spatial-temporal distributions of different velocity components. The notations u, v and w are the perturbation velocities in the x-, y-, and z-directions respectively, measured as deviations from the local mean velocities in the undisturbed flow. Both spanwise and normal distributions were measured, in which a set of isocontours in planes (y,t) and (z,t) is referred to as a vertical and horizontal disturbance structure respectively. The isocontours represent, unless otherwise mentioned, the streamwise perturbation velocity.

In addition to the study of the disturbance flow field in space, both temporal and spatial Fourier decompositions were performed using the spanwise distributions of the u-velocity. The transformed distributions are displayed as amplitude spectra in the frequency (f) – spanwise wave number (β) domain. Neither f nor β $(= 1/\lambda_z)$ are normalized, and they take the units Hz and m^{-1} respectively. In order to provide the possibility for direct comparisons of amplitudes between different plots, the size of the transformed time and space domain is always kept constant. This was done by padding zeros in the spanwise direction, thus assuming that the disturbance velocity was negligibly small outside of the measured region.

3. Results

It can be assumed that the receptivity to vortical free stream disturbances is highly dependent on the flow close to the leading edge where the boundary layer originates. In order to have a well defined flow around the leading edge the pressure distribution was carefully adjusted to be as uniform as possible. The pressure variations, evaluated from Bernoulli's equation using U_0 measured near the edge of the boundary layer, were similar to the distributions reported by Westin *et al.,* (1994). The flow accelerates smoothly from zero at the stagnation line to the outer velocity over a streamwise distance of about 20 mm, without producing any suction peak in the region close to the leading edge. The pressure variations along the plate were within 1% of the dynamic pressure, and the mean profiles were in close agreement with the Blasius distribution.

3.1. Characteristics of the disturbance close to the leading edge

When the short duration electric pulse forces the loud speaker membrane to move outwards, an air volume will be expelled from the pipe. It can be assumed that the initial phase of the jet excites a vortex ring which interacts with the mean flow, whereupon the jet, which has a relatively long duration, is deflected and mixed with the free stream. Consequently, the resulting free stream disturbance is somewhat complicated. In this study the interaction between the jet and the free stream was not investigated in detail, however, the disturbance field in the leading edge region was mapped quite carefully. It should be mentioned that the initial disturbance showed a strong dependence on both the orientation of the pipe with respect to the free stream direction, and the relative amplitude of the disturbance and the outer velocity U_0. In this case we were interested in modelling free stream turbulence of the order of a few percent and a scale of the order of a few millimeter to be able to compare with the experiments of Westin *et al.,* (1994). In that experiment the FST-level (Tu) was approximately 1.5% at the leading edge, which would correspond to a typical peak-to-peak value of the most energetic eddies of roughly 10%. An appropriate localized disturbance was found through trial and error.

Figure 2 shows the distribution of the streamwise velocity disturbance u in the immediate vicinity of the leading edge of the plate. The disturbance at $x = -3$ mm consists of two distinct regions, where an interpretation

is that the front region is associated with the starting vortex expelled from the pipe. As will be seen later, this part seems to have a passive role during the excitation of the boundary layer. The disturbance is symmetric around $z = 0$, and the spanwise scale, based on contours of $0.02U_0$, is approximately 2 mm. The second part of the disturbance has a duration of the order of 3 ms, which, if the disturbance travels with the free stream velocity, corresponds to a length of approximately 20 mm. Hence the aspect ratio (length-to-width) of the initial disturbance is of order 10, which is not correctly represented in the figure. In the vicinity of the pipe the perturbation amplitude was rather high, and the peak values for the positive and negative deviations at $x = -7$ mm were $0.4U_0$ and $-0.3U_0$ respectively (not shown). However, the strength of the u-disturbance decays rapidly towards the leading edge, and at $x = 3$ mm the peak-to-peak amplitude of the disturbance was about 10%.

The leading edge divides the impinging outer disturbance into two parts, however, this division was not found to result in qualitative changes of the streamwise velocity perturbation. As can be observed in Figure 2, the u-distributions at $x = 3$ and 7 mm are similar to the upper part of the disturbance at $x = -3$ mm. Also

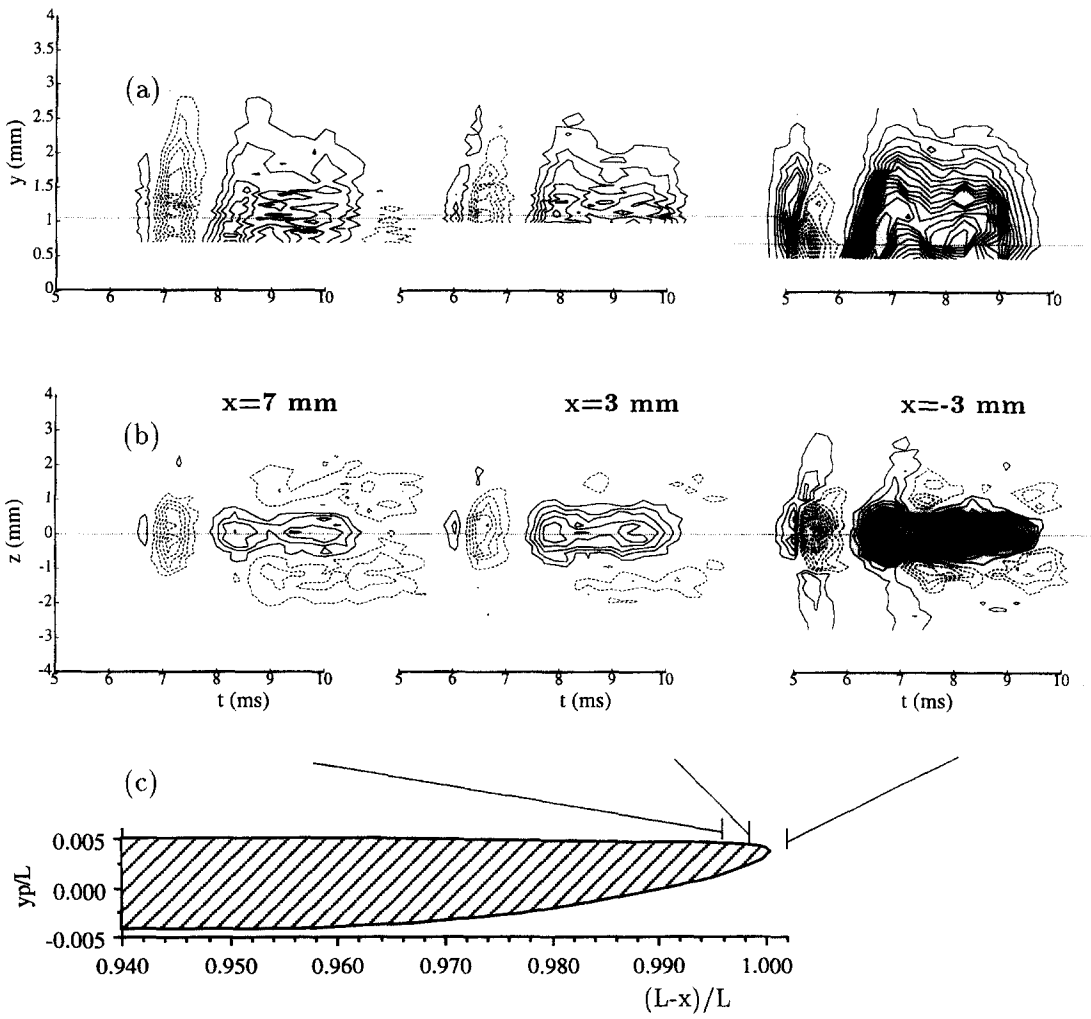

Fig. 2. – (a) Vertical and (b) horizontal distributions of u at three different x-stations in the vicinity of the leading edge. Contour spacing: $0.01U_0$. Vertical distributions measured in the symmetry plane (z=0), and horizontal distributions at $y = 0.7 - 1.1$ mm. The leading edge of the experimental test plate is shown for reference (the coordinate y_p is related to the leading edge. Reference length $L = 2.0$ m).

the spanwise scale of the disturbed region as well as the duration time are conserved as the disturbance is convected in the x-direction. A general trend that can be observed from the three x-stations is that the negative region in the front part of the disturbance becomes more prominent downstream, *i.e.* the decay of this region is slower than for the rest of the disturbance. As a matter of fact this negative perturbation could be observed far downstream, long after the positive part had disappeared.

It should be noted that in the vicinity of the pipe the repeatability of the hot wire signal was very good. This demonstrates that the generation of the vortical perturbation in the outer flow was stable and deterministic. However, at $x = 3$ mm differences were observed between single realizations, although the averaged flow structure at $x = 3$ mm are similar to that at $x = -3$ mm. This may result from a large sensitivity to small vertical displacements of the incoming disturbances with respect to the stagnation line.

Figure 3 shows the spanwise and vertical distributions of both u and v at $x = 3$ mm. The structure consists mainly of a central part with negative v on the symmetry plane ($z = 0$), *i.e.* flow towards the plate, whereas at each side there is a region of positive v. Such a distribution of v indicates streamwise vorticity, and this part of the external vortical perturbation may be interpreted as two counter rotating streamwise vortices. It should be noted that a similar distribution was observed also at a position just upstream of the leading edge. Consequently,

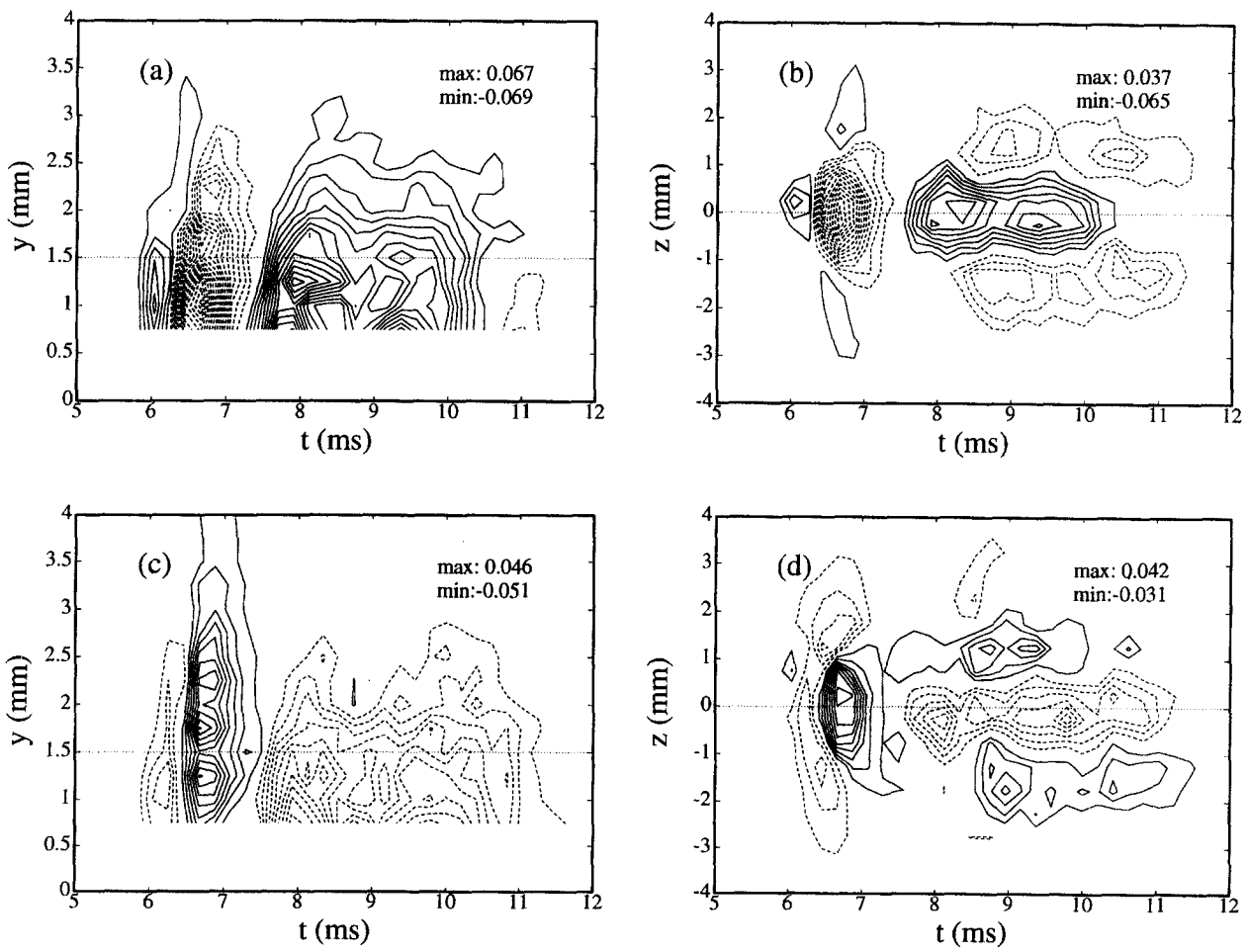

Fig. 3. – Spanwise and vertical distributions of the disturbance velocity at $x = 3$ mm. (a), (c) u- and v-distributions in the symmetry plane $z = 0$; (b), (d) u- and v-distributions in the horizontal plane at $y = 1.5$ mm. Contour spacing: $0.005U_0$.

the streamwise vorticity in the rear part of the disturbance is generated close to the disturbance source. Further, the front part of the disturbance is dominated by a positive v-component.

3.2. Generation of boundary layer disturbances

The first position where velocity measurements inside the boundary layer are shown is at $x = 15$ mm, where the boundary layer thickness was approximately 0.8 mm (*fig.* 4). In the (y,t)-planes (*fig.* 4a) the undisturbed mean profile is plotted together with profiles showing the maximum positive and negative disturbance levels normalized with the maximum absolute value. Similar curves are shown for the (z,t)-planes (*fig.* 4b). Both the vertical and horizontal u-velocity distributions reveal a strong boundary layer perturbation in the u-component, and the boundary layer becomes dominated by high and low velocity regions forming a streaky pattern.

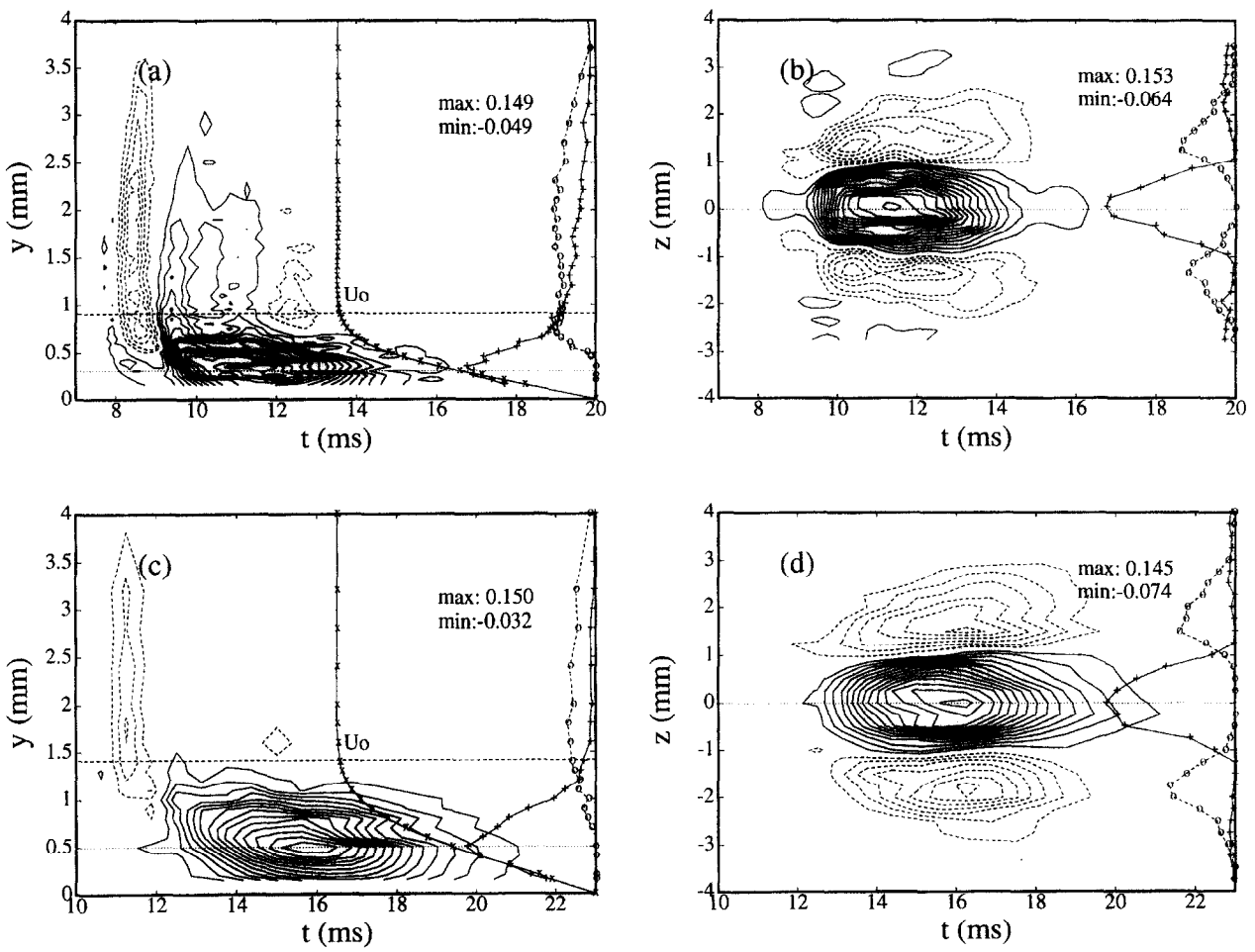

Fig. 4. – Distribution of u in the boundary layer. $x = 15$ mm (y,t)-plane at $z = 0$ (a), (z,t)-plane at $y = 0.30$ mm (b); $x = 35$ mm (y,t)-plane at $z = 0$ (c), (z,t)-plane at $y = 0.50$ mm (d). Contour spacing: $0.01U_0$. Labels: undisturbed mean velocity profile (×), undisturbed boundary layer edge (- - -), maximum negative (o) and positive (+) disturbance amplitude (same labels will be used in subsequent plots).

Further downstream (*fig.* 4c, d), at $x = 35$ mm, only the front part of the initial structure can be observed in the outer flow, while the positive perturbation has been completely damped out. This low velocity region can be considered as a reminiscence from the free stream disturbance impinging upon the leading edge. Inside the

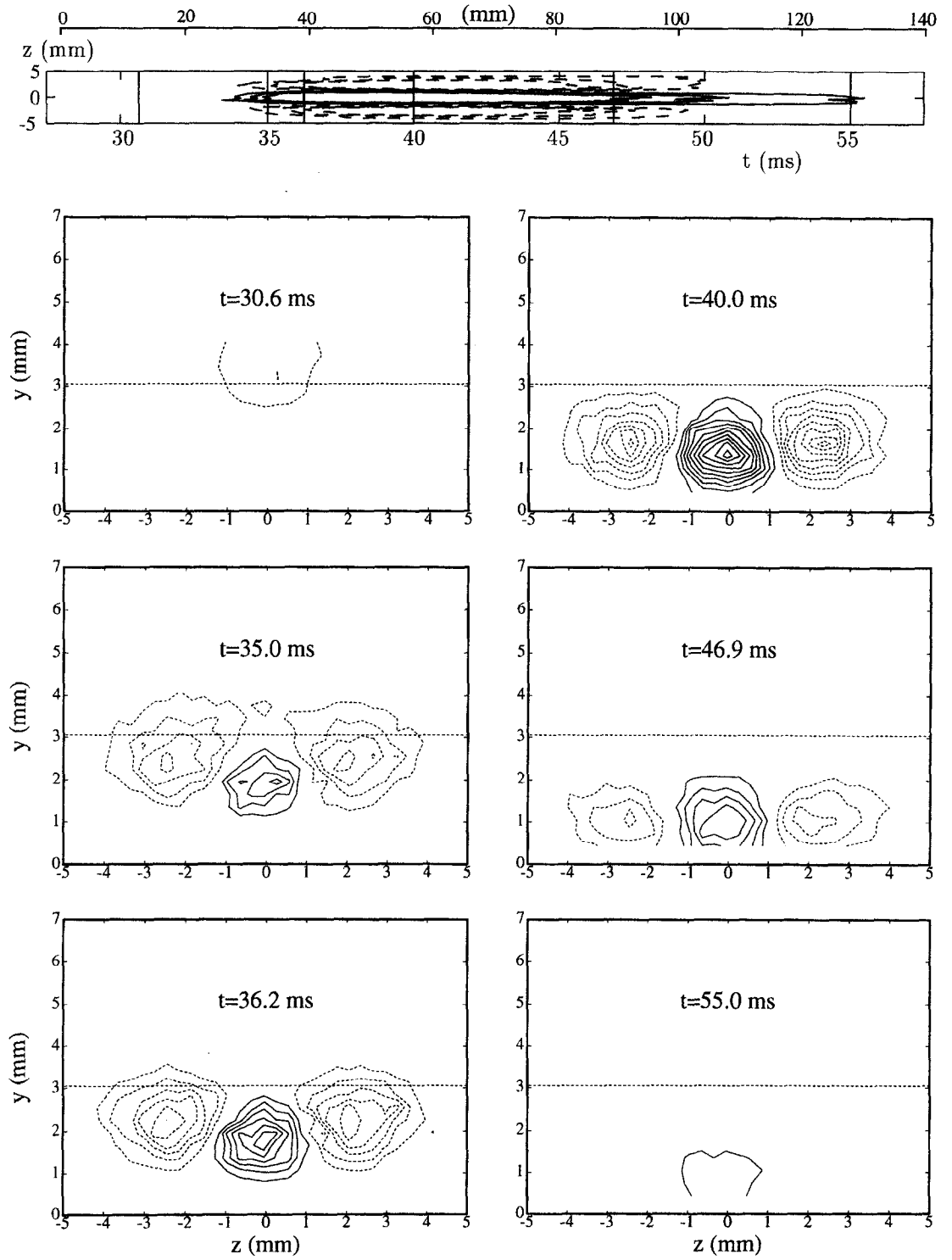

Fig. 5. – Cross-sections ((y,z)-planes) of the streamwise velocity perturbation at x = 160 mm. Contour spacing: $0.005U_0$. Dashed lines denote the boundary layer edge. Time is indicated in each figure and marked in the (z,t)-plane in the top figure. (Note that the upper horizontal axis in the top figure is plotted to approximately show the correct length-to-width ratio of the localized boundary layer disturbance; the chosen propagation speed was 0.7 U_0 (*see* fig. 8)).

boundary layer the perturbation has qualitatively the same shape as in Figure 4b, but the dominant contribution to the velocity signal was more deterministic at $x = 35$ mm than the signals measured at $x = 15$ mm. In contrast to the free stream disturbance, the intensity of the induced u-perturbations is almost the same at both x-positions (peak-to-peak amplitude about 24%), although the overall size of the whole structure increases downstream. This points out that the total disturbance energy inside the boundary layer has grown between the two stations. The maximum absolute value of the perturbations in the negative regions are positioned further out in the boundary layer compared with the maximum positive perturbation on the centreline, and the perturbation also extends outside the boundary layer edge (not shown). The overall picture is similar to the disturbance that can be expected from two counter rotating streamwise vortices, with an upward movement of low-velocity fluid from the near wall region on either side of the centreline, and a displacement of high velocity fluid towards the wall at $z = 0$.

More extensive measurements were carried out at $x = 160$ mm, where the (y, z)-plane was mapped as the disturbance passed by. The spanwise distribution of the boundary layer disturbance shown in Figure 5 is plotted with approximately correct length-to-width ratio of the localized disturbance, and the long and narrow shape of the streaks becomes evident. The spanwise scale of each streak is approximately equal to the wall-normal one, which is of the order of the boundary layer thickness. At $t = 30.6$ ms the negative streamwise velocity region is just above the outer edge of the boundary layer, which is associated with the front part of the incoming external perturbation. As was stated above this part does not penetrate into the boundary layer, but is convected with the free stream velocity outside the boundary layer edge.

For the cross sections measured in the rear part of the disturbance the positive region becomes more manifested, and the position with maximum disturbance amplitude is found approximately at $t = 40$ ms. It is also evident from Figure 5 that the structure is inclined with respect to the wall.

It has been mentioned that the overall picture of the disturbance resembles the effect of two counter rotating streamwise vortices. In order to find out if there was a streamwise vortical motion in the boundary layer, qualitative measurements of the w-component were carried out at $x = 160$ mm. These measurements were undertaken in the same manner as by Henningson and Alfredsson (1987), using first a standard single wire probe, followed by measurements with a probe with a slanted wire. The measurements were carried out in the vertical planes between the positive and negative regions. These are the positions where a maximum spanwise velocity component can be expected, which in case of streamwise vortices should be directed both in positive and negative directions in each cross-section. The results showed a spanwise component directed outwards from the centreline in both cross-sections, but no sign of a vortical motion could be observed (although this does not exclude that streamwise vorticity is present). It is therefore assumed that a vortical motion is only present in the region close to the leading edge, where it sets up the observed high and low velocity streaks. The streaks attain rapidly large amplitudes in the u-component, which can be observed far downstream, although the initial vortical motion is damped out.

3.3. Spatial evolution of the boundary layer disturbance

Figures 6 and 7 show the evolution of the streamwise velocity perturbations in (y, t)- and (z, t)-planes at several x-locations. The amplitude is decreasing as the boundary layer structure moves downstream, and the spanwise scale is seen to increase slightly. Close to the plate surface the excess velocity region in the plane of symmetry, $z = 0$, and defect velocity regions on either side of the centreline, propagate more slowly than at the outer edge of the boundary layer. This leads to an elongation of the structure in the streamwise direction. It should be emphasized that both the normal and spanwise scale of the disturbance, which are of the order of the boundary layer thickness, is much smaller than the streamwise scale, although it is not evident from the presented u-velocity distributions (compare *fig.* 5).

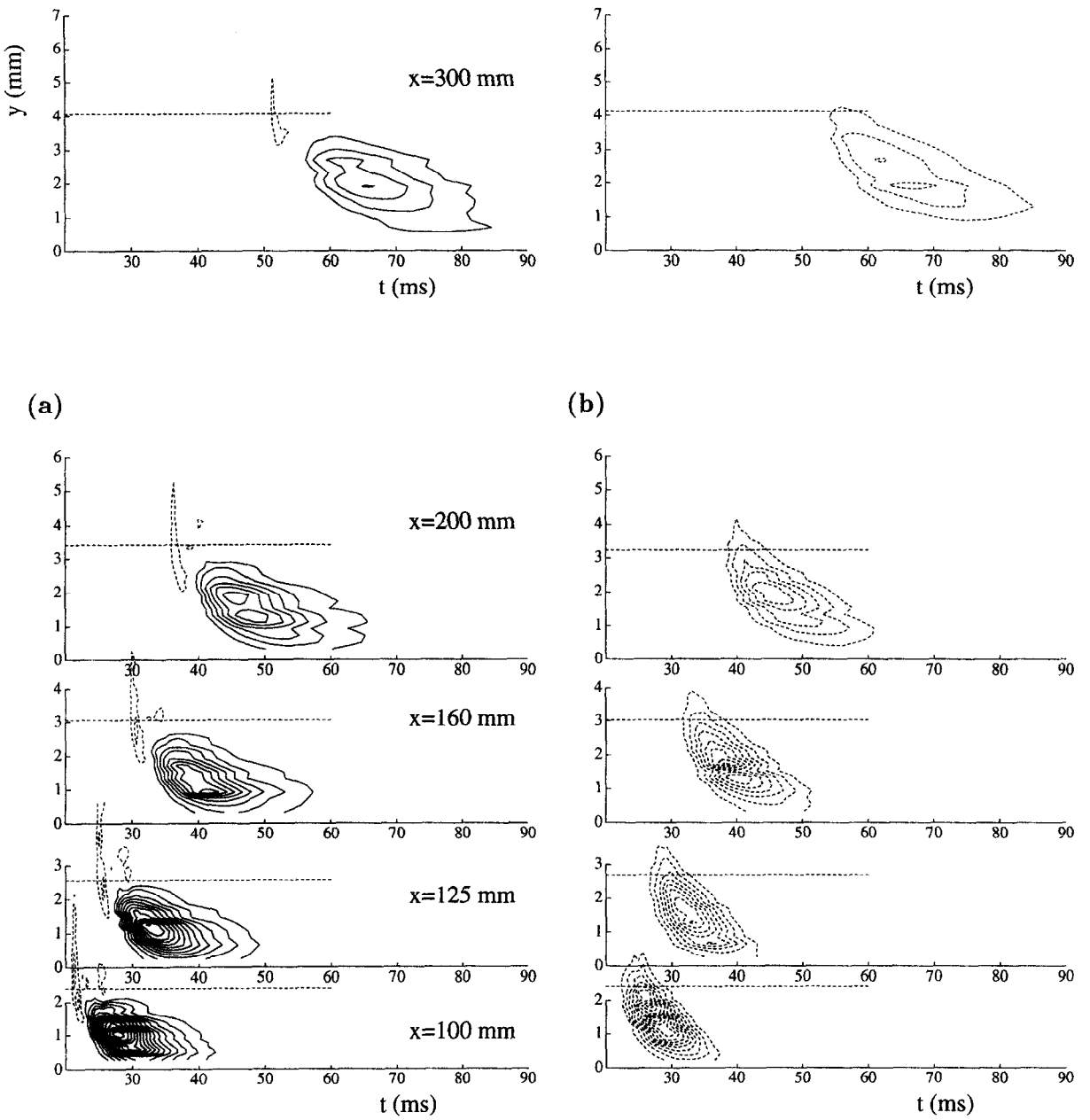

Fig. 6. – Vertical distributions of u measured at different streamwise positions. (a) symmetry plane (z=0); (b) z-locations with maximum negative disturbance amplitude. Contour spacing: $0.005U_0$. Dashed lines denote the boundary layer edge.

From the figures it seems that the propagation speed for various parts of the disturbance are different but constant. The foremost part of the boundary layer structure propagates at approximately $0.9U_0$, which almost corresponds to the local mean velocity. In order to obtain an objective measure of the propagation speed of the disturbance, it was followed along lines with constant mean velocity ($U = 0.25, 0.50, 0.75, 0.85, 0.90U_0$), and the structure was identified by various values of the streamwise disturbance velocity (0.1, 0.3 and 0.5 of maximum u at each x). The results from this evaluation is shown in Figure 8 for the front and rear part of the

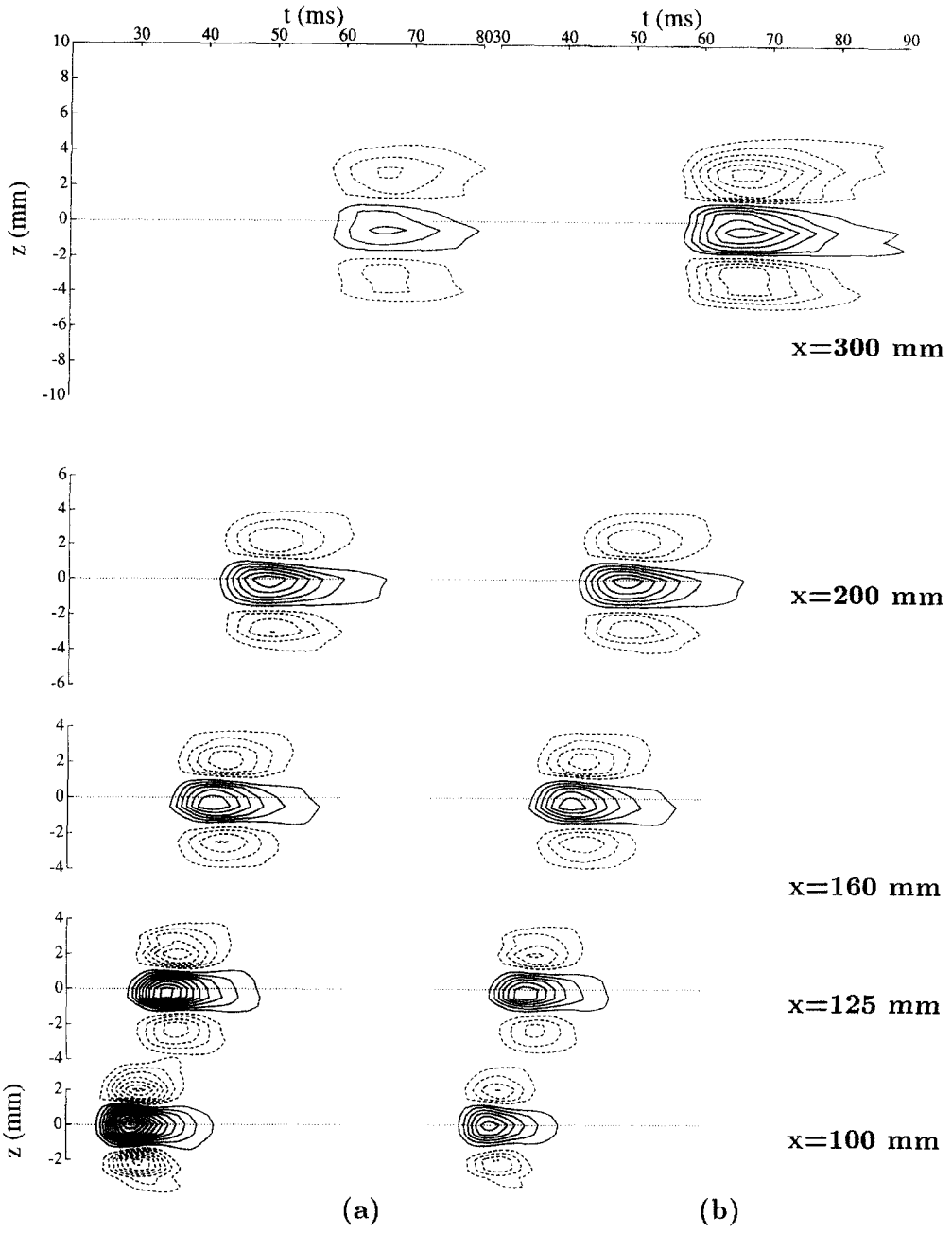

Fig. 7. – Spanwise distributions of u measured at $y/\delta^* \approx 1 - 1.5$ at different x-positions.
(a) contour spacing: $0.005U_0$; (b) contour spacing: 15% of the maximum positive peak amplitude at each x-position.

disturbance. It is clear that the front of the disturbance propagates at a higher velocity than the corresponding local mean velocity, independent of the level or y-position chosen. This velocity is relatively constant across the major part of the boundary layer ($0.8 - 0.9U_0$), which implies that close to the wall the propagation speed is several times the local mean velocity. The propagation speed of the rear part is also rather constant across the boundary layer ($0.5 - 0.7U_0$), which means that it propagates slower than the mean flow in the outer part of the boundary layer and faster in the vicinity of the wall. The propagation speeds shown in Figure 8

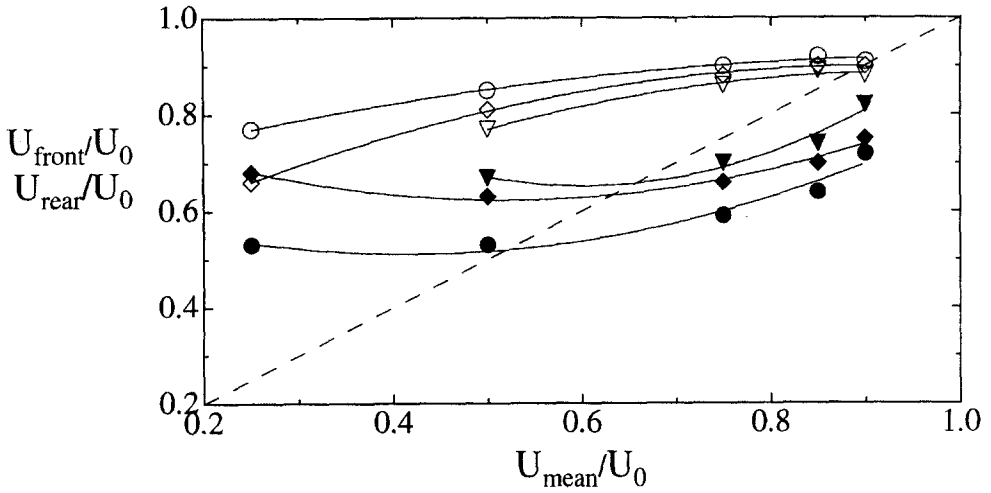

Fig. 8. – Propagation speed of the front (open symbols), and rear (filled symbols) interface of the boundary layer disturbance based on different contour levels. 10% of the maximum peak value of the positive velocity deviation (○); 30% (◇) and 50% (▽). Propagation speeds extracted at five different y-locations are shown. The dashed line represents a velocity equal to the local mean velocity inside the boundary layer.

were extracted in the plane of symmetry ($z = 0$), but a similar evaluation in the negative regions beside the centreline gave almost identical values.

Although the major part of the results were obtained at a fixed initial amplitude and a fixed position of the pipe, some tests were carried out with a smaller initial amplitude. In Figure 9 the original disturbance is compared with a boundary layer disturbance having an amplitude about twenty times smaller than the original one. Both disturbances show some similarities, with one positive and two negative streaks. It should be noted that the contour spacing is smaller in Figure 9c, which can at least partly explain why the streamwise extent of the boundary layer disturbance is larger for the lower amplitude. However, it is obvious that also the spanwise distance between the negative streaks is larger for the lower amplitude, which must be due to either a different spanwise scale of the initial disturbance, or a difference in how the disturbance is transformed into the boundary layer. It can also be observed that the propagation speed of the front part and the region of maximum perturbation amplitude are almost the same for both cases. The rear part is less distinguishable, giving different propagation speeds for different choices of iso-contours. However, by choosing a small disturbance level for both cases ($0.00025U_0$ in Figure 9) the disturbed regions are almost equal in size.

3.4. Spectral behaviour of the localized disturbance

Spectral decompositions of the ensemble averaged spanwise distributions of u at $x = -3$, 35 and 160 mm are shown in Figure 10 for both the large and the small amplitude disturbance. At the first x-position the perturbation energy for the disturbance of large initial amplitude is spread over a wide range of frequencies (0-1000 Hz) and spanwise wave numbers. At $x = 35$ mm, the spectrum inside the boundary layer is dominated by two peaks at a spanwise wave number of 235 m^{-1}. This corresponds to a spanwise wavelength (λ_z) of 4.3 mm. Further downstream ($x = 160$ mm), the spectrum shows a concentration of energy to lower frequencies, dominated by a spanwise wave number of 165 m^{-1} ($\lambda_z = 6.1$ mm). These results are in agreement with observations made in the (z,t)-planes.

For the case with a smaller initial amplitude, the influence from background disturbances becomes larger. However, the main difference is the smaller spanwise wave number that is observed for the major peaks in

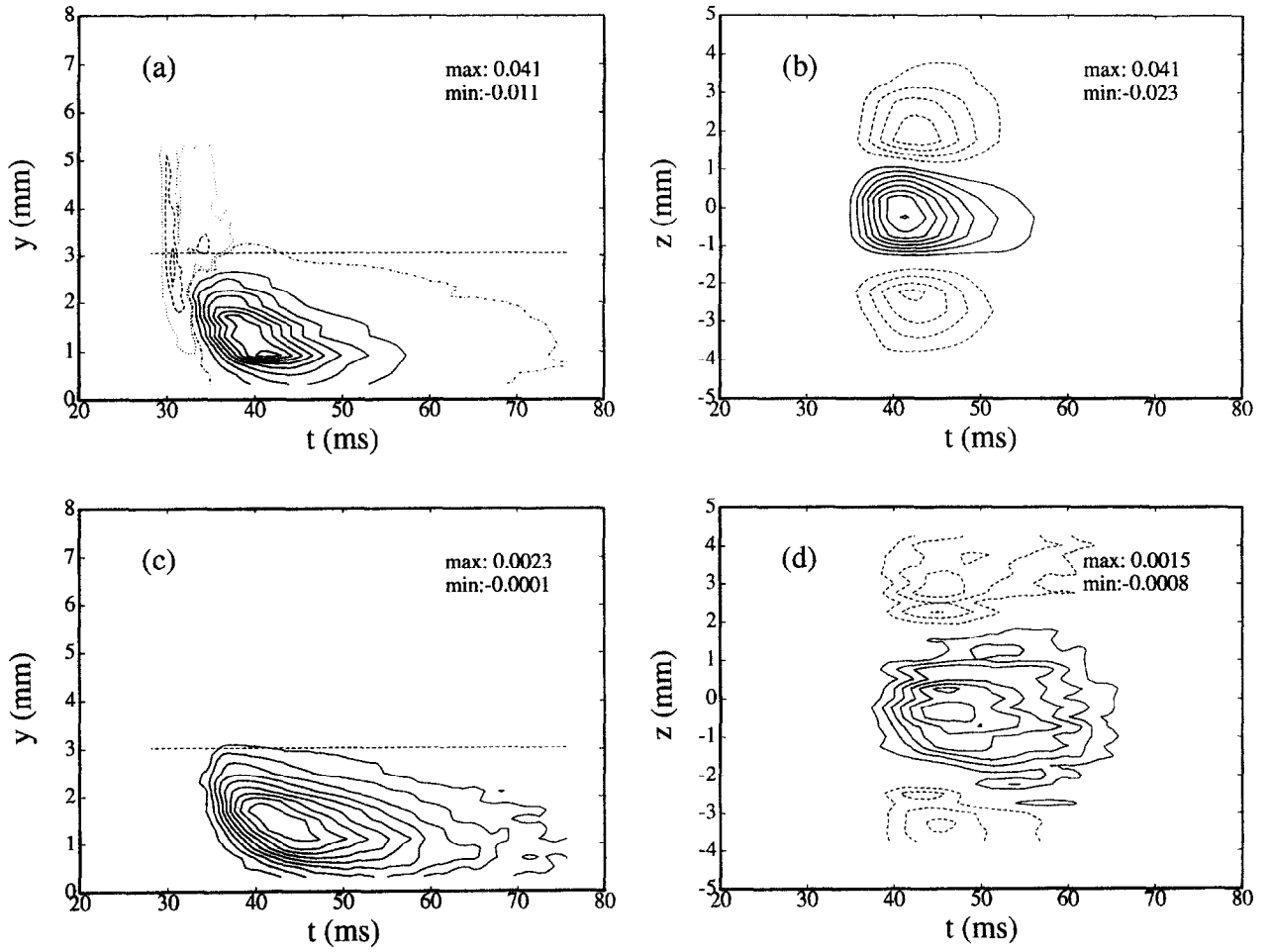

Fig. 9. – Boundary layer disturbances obtained for two different initial amplitudes. (x=160 mm). Strong disturbance: (a) (y,t)-plane at z=0, (b) (z,t)-plane at y=0.92 mm. Contour spacing: $0.005U_0$; (one positive and negative contour with a level of $0.00025U_0$ are also shown in (a)). Weak disturbance: (c) (y,t)-plane at z=0, (d) (z,t)-plane at y=0.82 mm. Contour spacing: $0.00025U_0$.

the spectrum, which is in agreement with the larger spanwise distance that was observed between the negative streaks in Figure 9.

From the Fourier decompositions of the disturbed flow fields, the spanwise wavelength corresponding to the most energetic spectral component is extracted and plotted as function of the Reynolds number (*fig.* 11a) Also the growth of the boundary layer thickness δ_{99} (δ_{99} is defined as the y-position where $U = 0.99U_0$) and the development of the ratio λ_z/δ_{99} are shown in the same figure. It should be noted that δ_{99} is extracted from the undisturbed boundary layer, and the ratio between δ_{99} and the displacement thickness (δ^*) is relatively constant for different x, with a value close to what can be expected in a Blasius boundary layer (2.8-2.9). The ratio of λ_z/δ_{99} plotted in Figure 11a seems to approach a value close to 2 for large Reynolds numbers. However, the spanwise spreading rate can be estimated from Figure 11b, in which the same quantities are plotted in a logarithmic scale. As expected, δ_{99} grows proportional to $x^{0.5}$. The development of λ_z shows a smaller growth rate, and a curvefit to the linear region in Figure 11b gives an exponent close to 0.2. Consequently, there is no evidence from the present data that the ratio λ_z/δ_{99} should approach a constant value.

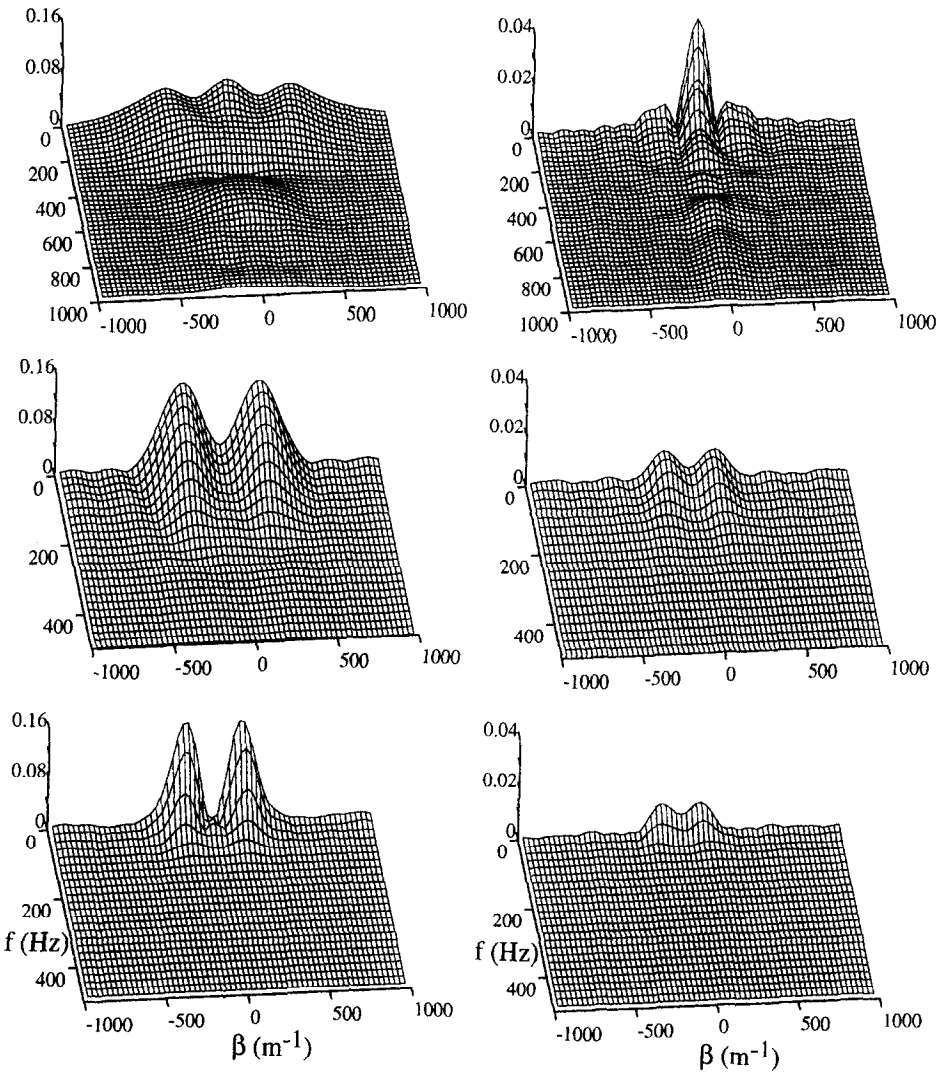

Fig. 10. – Spectral decomposition (f, β) for different spanwise distributions. The x-positions are from top to bottom -3 mm (free stream), 35 mm and 160 mm (the last two distributions measured at $y \approx \delta^*$). Left and right column correspond to large and small initial amplitude respectively.

In Figure 12a the amplitude development of different frequency components are displayed, which are extracted from the dominating spanwise wave number (β_{max}) at each x-station (β_{max} decreases downstream). Also the normalized values of the positive and negative peak amplitudes, normal-vorticity components (approximated with $\partial u/\partial z$) and the total rms-level in the spectra are shown in Figure 12b. The last quantity can serve as a measure of the total disturbance energy in the considered (z, t)-cross-section of the disturbance. It should be emphasized that some arbitrariness is introduced, since only one spanwise plane is considered at each x-station, instead of measuring the complete structure to get the total disturbance energy. However, the cross-sections were chosen at y-positions corresponding to the maximum positive perturbation velocity on the centreline ($y/\delta^* \approx 0.9 - 1.4$).

Nevertheless, it is interesting to note that the maximum perturbation amplitude and the total rms-level start to decrease after an initial region of growth, while the component corresponding to $(f, \beta) = (0, \beta_{max})$ remains fairly constant as the disturbance propagates downstream. Consequently, higher harmonics damp faster, and the concentration of energy to low streamwise wave numbers corresponds to long, persistent streaky structures in

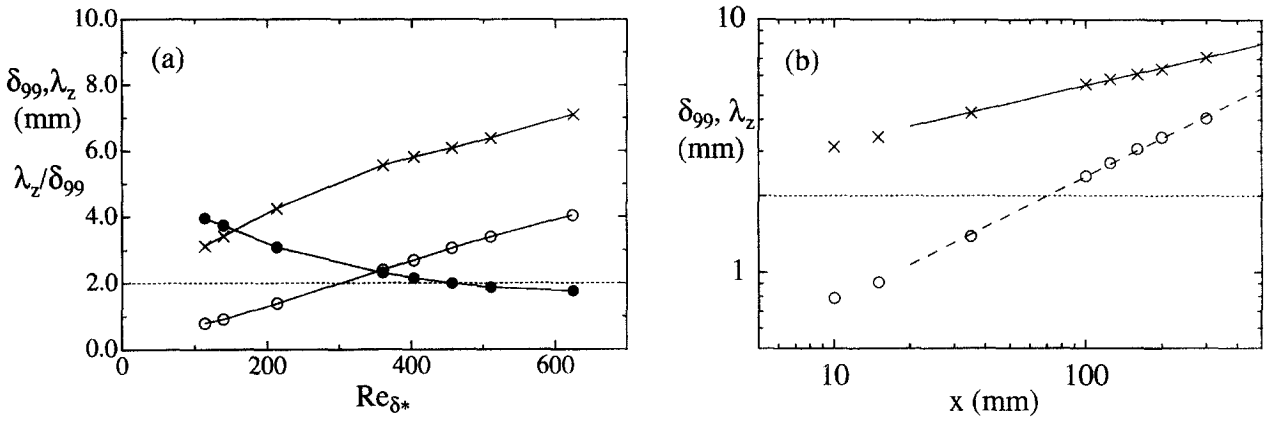

Fig. 11. – (a) Downstream development of the boundary layer thickness (δ_{99}) (o), dominant spanwise wavelength (λ_z) (×) and the ratio λ_z/δ_{99} (•). (b) Labels as in figure (a) but plotted with a logarithmic scale. Solid line shows a curvefit to λ_z in the range $x \in [35, 300]$ mm, and the dashed line corresponds to $x^{0.5}$.

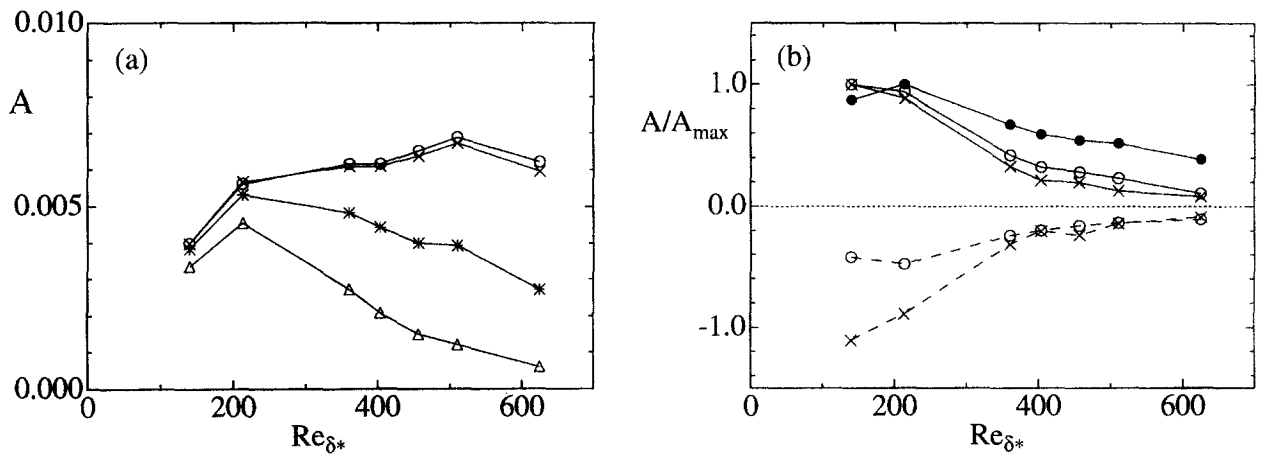

Fig. 12. – (a) Downstream development of the amplitude of different spectral components extracted for $\beta=\beta_{max}$ at each streamwise position ($y/\delta^* \approx 0.9 - 1.4$): f=0 (o), f=6.25 Hz (×), f=31.25 Hz (*) and f=62.5 Hz (△). (b) Downstream development of different quantities: u_{rms} (•); $(u)_{max}$ (— o —); $(u)_{min}$ (– – o – –); $(\partial u/\partial z)_{max}$ (— × —); $(\partial u/\partial z)_{min}$ (– – × – –). All curves are normalized with the maximum positive value of each quantity.

the flow. As can be expected, the decay of the normal vorticity starts further upstream than the decay of the maximum amplitude, since also the spanwise growth of the structure reduces the magnitude of $\partial u/\partial z$.

3.5. Comparisons with measurements at moderate levels of free stream turbulence

The purpose of the present study was primarily to generate a controlled disturbance in the free stream that could serve as a model for studies of the receptivity process at moderate and high levels of free stream turbulence (FST). A general observation in a laminar boundary layer subjected to FST is the formation of longitudinal, streaky structures. These unsteady streaks cause low-frequency fluctuations in the u-component, with the maximum amplitude positioned approximately in the middle of the boundary layer. The u_{rms}-level grows during the downstream development, and can attain amplitudes of the order of 10% before transition occurs. Furthermore, the fluctuations give rise to small but characteristic modifications of the mean velocity profiles, although the displacement thickness is almost unaffected. Normalized profiles of the mean velocity

deviation (i.e. the deviation from the corresponding profile measured at a low FST-level) and u_{rms} obtained from measurements at a free stream turbulence level (Tu) of 1.5% are shown in Figures 13a and b (*see* also Westin *et al.*, 1994).

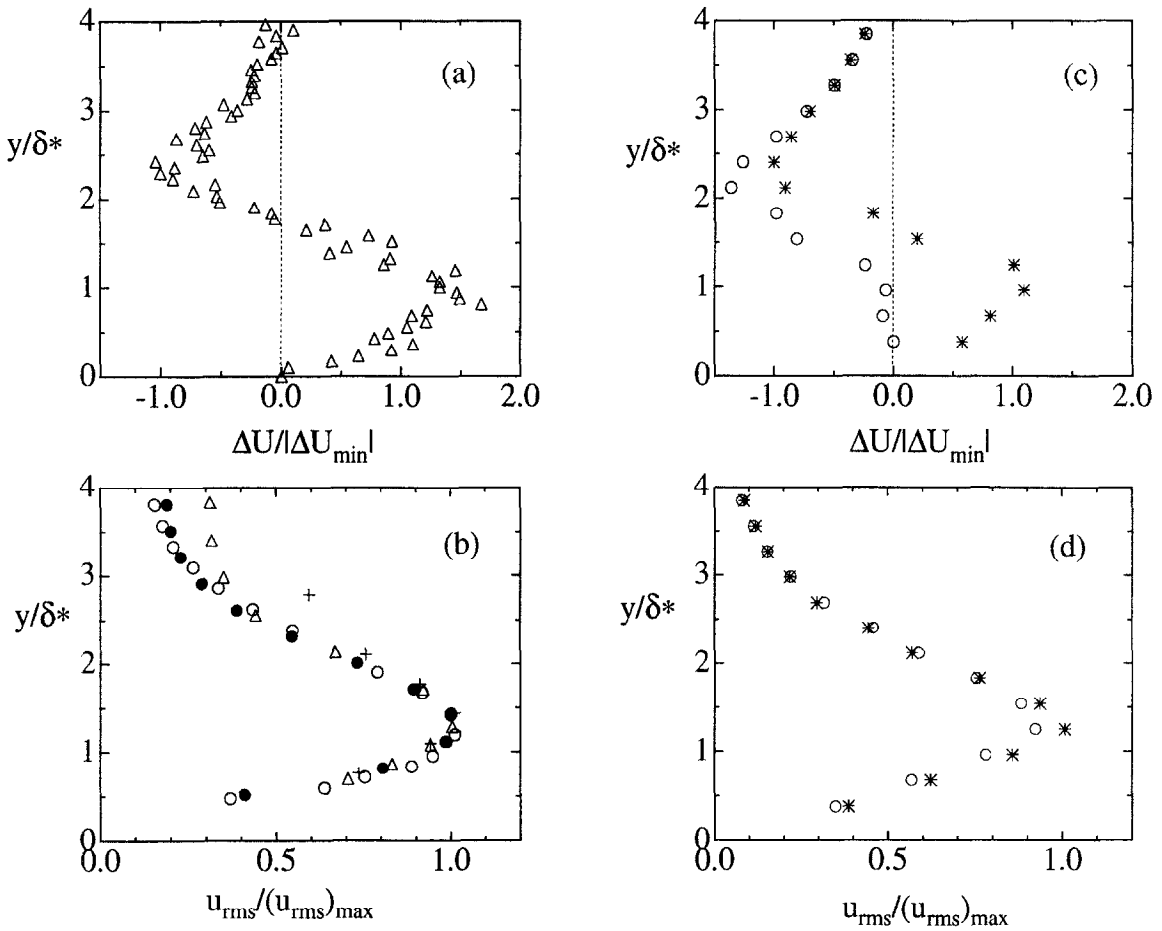

Fig. 13. – Influence of free stream turbulence (Tu=1.5%; U_0=8 m/s): (a) mean velocity deviation at x=450 mm, normalized with the minimum, and (b) normalized profiles of u_{rms} measured at different downstream positions. (c) Mean velocity deviation and (d) u_{rms} extracted from the localized disturbance at x=160 mm by averaging over t and z. Averaging over a spanwise distance corresponding to two ($*$) and three ($\circ$) streaks, respectively. The curves are normalized with the minimum in ΔU (c) and maximum in u_{rms} (d) obtained when averaging over two streaks.

In the present experiment the localized free stream disturbance transferred into longitudinal streaky structures inside the boundary layer, resulting in large streamwise perturbation amplitudes. For comparison with the profiles in Figures 13a and b, similar profiles were extracted from the localized disturbance shown in Figure 5c (x = 160 mm). Each point in the y-direction was obtained by averaging in both time and the spanwise direction. The spanwise averaging was carried out either over the total extent of the disturbance, or in a region restricted to one positive and one negative streak. As can be observed from Figure 13c, the averaging over only two streaks gives a shape of the mean velocity deviation in close agreement with the profiles obtained in the FST-case. The location of the zero-crossing, the wall-normal extent of the disturbed region as well as the relative ratio between the negative and the positive deviation show apparent similarities. The corresponding plots of the extracted u_{rms}-profiles show a smaller dependence on the size of the averaged domain, and also in this case the shape and the location of the maximum are in quite good agreement with the profiles measured at a moderate level

of free stream turbulence. The primary aim with the plots is to show the similarity in the profile shapes, and a direct comparison of the magnitudes of ΔU_{min} can also be somewhat misleading. The Reynolds numbers are very different, and, as pointed out above, the downstream development is different in the two cases (increasing and decreasing amplitudes respectively). Moreover, the value calculated in Figure 13c is an average over z and t, which means that the magnitude will depend on how large a domain (in z and t) is chosen. However, it can be mentioned that the instantaneous peak deviations are of the order of 5% in Figure 5, and the value of ΔU_{min} in Figure 13a is about 0.8% of U_0.

It should be emphasized, however, that although non-stationary, longitudinal streaks can be observed in a boundary layer subjected to free stream turbulence, they are mixed with other types of disturbances. Consequently, one should expect differences compared with the simplified case with a set of isolated streaks in the boundary layer. With this in mind, it is encouraging that many of the characteristics of the time averaged profiles in the case of FST also can be recognized in the simple structure that is generated in the present study.

4. Discussion

An attempt to illustrate the receptivity process in the present experiment is shown in Figure 14. The interpretations are based on the present experimental results, as well as some general findings from studies on transient growth (cf. section 1.3). As pointed out earlier the rear part of the free stream disturbance, which

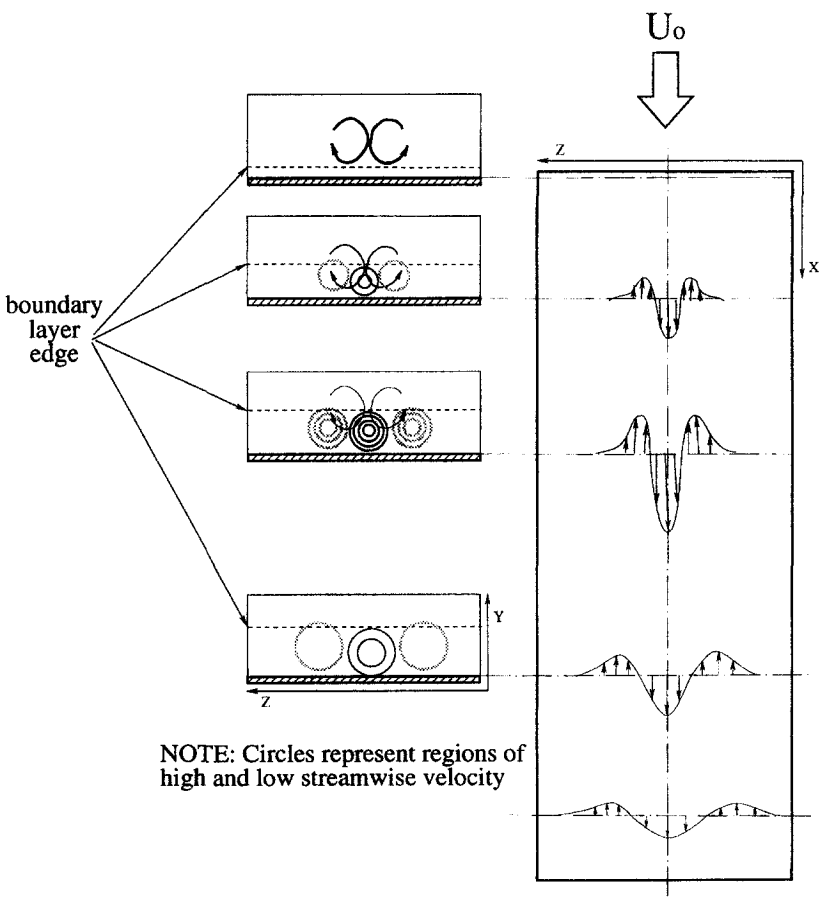

Fig. 14. – Illustration of the receptivity process.

turned out to be most efficient in exciting a boundary layer disturbance, is interpreted as two counter rotating streamwise vortices. When the vortical motion interacts with the thin boundary layer close to the leading edge the negative v-velocity on the centreline and the positive one aside of the centreline will displace fluid in the wall-normal direction, and thus generate perturbations in the streamwise component. Although the strength of the free stream disturbance is continuously decreasing downstream, the result will initially be an increasing perturbation amplitude in u. However, after a relatively short downstream distance the wall-normal motion will be too weak, and a downstream decay of the u-perturbation will follow after the transient growth.

One of the major objectives with the present experiment was to generate a disturbance which could serve as a model for FST-induced boundary layer perturbations. Although several similarities concerning the disturbance characteristics can be observed, one important difference remains, namely the decay of the localized disturbance in contrast to the growing rms-fluctuations in the case of FST. This difference can not be explained based on the present results, but some ideas will be given below. If it is assumed that the initial growth in amplitude of the streaks can be described by transient growth due to lift-up, the relatively low Reynolds-numbers close to the leading edge will bound the maximum energy growth. However, once the streaks have been generated, the continuous forcing from the free stream turbulence may promote the energy growth of the existing streaks, which grow in amplitude downstream. For instance, pressure fluctuations due to the larger vortices in the free stream, or direct action from free stream vortices penetrating the boundary layer edge, may enhance the perturbation amplitude of the streaks. Also, interactions between adjacent streaks as well as other types of disturbances inside the boundary layer may play a role for the downstream development. A downstream growth of the streamwise perturbation amplitude inside the boundary layer was observed by Bertolotti and Kendall (1997), who studied the response to a stationary free stream vortex. The difference, as compared to the present experiment, might be explained by the relatively slow downstream decay of the vortex strength, which results in a long region of forcing of the boundary layer.

Another, slightly different scenario, is that streaks are continuously generated and damped as the flow develops downstream. Since the Reynolds number increases, the streaks that are generated further downstream can achieve a larger transient energy growth, resulting in an increased u_{rms}-level. However, the growing boundary layer thickness, as well as the decaying amplitude of the free stream turbulence, will both reduce the direct effect of lift-up. Although the two suggested scenarios differ concerning the endurance of the streaks, they both emphasize the importance of a continuous influence from the FST along the boundary layer edge.

An issue of interest is also the possible existence of a preferred spanwise wave length in the boundary layer. In recent experiments carried out in Novosibirsk (Bakchinov *et al.*, 1997) localized disturbances were introduced in a flat plate boundary layer by means of short-duration suction and injection of air through different slots positioned at subcritical Reynolds numbers. It was found that at subcritical initial amplitudes, *i.e.* amplitudes for which the disturbance did not immediately evolve into a turbulent spot, all disturbances developed longitudinal structures similar to those observed in the present work. The disturbances slowly decayed downstream and did not break down into turbulent spots within the considered Reynolds number range. After an initial phase of formation, the energy of all localized disturbances were centred at low frequencies (low streamwise wave numbers) and at non-zero spanwise wave numbers. Two "preferable" spanwise wavelengthes of the longitudinal structures were found, approximately 2 and 5-6 (normalized with the local boundary layer thickness). Which of these two wavelengthes that became dominant were dependent on the initial amplitude and the spectral composition of the initial disturbance. Flow visualizations of a boundary layer subjected to free stream turbulence by Alfredsson *et al.*, (1995) in the MTL-wind tunnel have also shown that variation of the free stream velocity resulted in different spanwise scales inside the boundary layer. Consequently, there seems to be a dependence on the relation between free stream scales and the boundary layer thickness. On the other hand, relatively weak selection of scales is observed in local analysis of transient growth (Butler

and Farrell, 1992), stability calculations with Parabolized Stability Equations (Herbert and Lin, 1993), as well as in Direct Numerical Simulations by Berlin and Henningson (1994). In the latter study oblique waves were introduced in the free stream, which generated streamwise streaks inside the boundary layer. By varying the wave angles, and thus the spanwise scale of the induced streaks, it was shown that the energy growth depend on the spanwise scale, although the spanwise wave number corresponding to the maximum growth was not strongly preferred. However, there are few experimental studies related to receptivity of boundary layers to external vortical perturbations of moderate and high amplitudes, and it is too early to draw a definite conclusion about the selection of a preferred spanwise scale inside the boundary layer.

5. Summary and conclusions

The results obtained in the present study can be summarized as follows:

(i) A complex transient free stream perturbation has been used to generate a localized boundary layer disturbance. The latter shows a simple structure, consisting of long and narrow streaks of positive and negative perturbations in the u-component. Despite a large perturbation amplitude inside the boundary layer close to the leading edge, the disturbance decays downstream without causing transition.

(ii) The spanwise scale of the streaks as well as the averaged perturbation profiles show qualitative similarities with the disturbances that are induced in a laminar boundary layer subjected to moderate and high levels of free stream turbulence.

(iii) Although the present study is limited to a few different initial disturbances, the results indicate that the spanwise gradients of the wall-normal velocity component are crucial for the boundary layer receptivity. Also the sign of the wall-normal component might be important, where a negative v-component more easily penetrates the boundary layer than a positive one.

The present results support earlier findings that the wall-normal velocity component, in combination with a strong three-dimensionality, is most important for the boundary layer receptivity. Also the scale of the free stream disturbance seems to be important. Although one can expect that there exists a preferred spanwise wave length which results in maximum energy growth, the results indicate that the scale of the induced boundary layer disturbance is to a large extent dependent on the scale of the free stream vortex.

However, in the present experiment the disturbance, if left by itself, decays and other mechanisms have to be at play for by-pass transition to occur at these low Reynolds numbers. The continuous forcing by the FST is probably important, as it may excite instabilities on the streaky structures, as well as induce new perturbations inside the boundary layer. Random interaction between streaks may also be of importance, as well as interactions with TS-waves. The presently obtained structure can be useful in order to model interactions between different types of disturbances, since it is a controlled disturbance which exhibits some of the characteristics observed in a transitional boundary layer. Additional experiments concerning the interaction between the present localized disturbance and periodical wave disturbances are reported in Bakchinov *et al.*, (1998).

Acknowledgements. – This work was supported by the Swedish National Board for Industrial and Technical Development (NUTEK). The visits to KTH of Prof. V.V. Kozlov and Dr. A.A. Bakchinov were made possible through exchange programs sponsored by the Royal Swedish Academy of Sciences (KVA), the Göran Gustafsson Foundation and the Swedish Institute (SI). Part of the evaluation of the data as well as preparation of the paper were carried out in Novosibirsk, and in that case sponsored by the Russian Basic Sciences Foundation, grant No 93-01-17359. S. Berlin, F. Bertolotti, D. Henningson and P. Luchini are acknowledged for useful discussions and comments.

REFERENCES

ALFREDSSON P. H., BAKCHINOV A. A., KOZLOV V. V., MATSUBARA M., 1995, Laminar-Turbulent transition structures at a high level of a free stream turbulence. In *IUTAM Symposium on Nonlinear Instability and Transition in Three-Dimensional Boundary Layers*, DUCK P. W., HALL P. Eds., Kluwer, 423–436.

ALFREDSSON P. H., MATSUBARA M., 1996, Streaky structures in transition, In *Proc. Transitional Boundary Layers in Aeronautics*, Henkes R.A.W.M., van Ingen J.L. Eds., Elsevier Science Publishers, 373–386.

AMINI J., LESPINARD G., 1982, Experimental study of an "incipient spot" in a transitional boundary layer, *Phys. Fluids*, **25** (10), 1743–1750.

BAKCHINOV A. A., WESTIN K. J. A., KOZLOV V. V., ALFREDSSON P. H., 1995, On the receptivity of a flat plate boundary layer to localized free stream disturbances, In *Laminar-Turbulent Transition*, Kobayashi R. Ed., Springer-Verlag, 341–348.

BAKCHINOV A. A., GREK G. R., KATASONOV M. M., KOZLOV V. V., 1997, Experimental study of localized disturbances and their development in a flat plate boundary layer, Preprint No. 1-97, ITAM, Russian Academy of Sciences, Novosibirsk, Russia (in Russian).

BAKCHINOV A. A., WESTIN K. J. A., KOZLOV V. V., ALFREDSSON P. H., 1998, Experiments on localized disturbances in a flat plate boundary layer. Part 2. Interaction between localized disturbances and TS-waves, *Eur. J. Mech., B/Fluids*, **17**, (6) 847–873.

BERLIN S., HENNINGSON D. S., 1994, A study of boundary layer receptivity to disturbances in the free stream, In *Bypass Transition - Proceedings from a Mini - Workshop*, HENNINGSON D. S. Ed., Stockholm, TRITA-MEK, Technical Report 1994, 14, 29–41.

BERTOLOTTI F. P., 1997, Response of the Blasius boundary layer to free-stream vorticity, *Phys. Fluids*, **9** (8), 2286–2299.

BERTOLOTTI F. P., KENDALL J. M., 1997, Response of the Blasius boundary layer to controlled free-stream vortices of axial form, *AIAA Paper 97-2018*.

BOIKO A. V., WESTIN K. J. A., KLINGMANN B. G. B., KOZLOV V. V., ALFREDSSON P. H., 1994, Experiments in a boundary layer subjected to free stream turbulence. Part 2. The role of TS-waves in the transition process, *J. Fluid Mech.*, **281**, 219–245.

BREUER K. S., HARITONIDIS J. H., 1990, The evolution of a localized disturbance in a laminar boundary layer. Part I: Weak disturbances, *J. Fluid Mech.*, **220**, 569–594.

BUTLER K. M., FARRELL B. F., 1992, Three-dimensional optimal perturbations in viscous shear flow, *Phys. Fluids A*, **4**, 1637–1650.

COHEN J., BREUER K. S., HARITONIDS J. H., 1991, On the evolution of a wave packet in a laminar boundary layer, *J. Fluid Mech.*, **225**, 575–606.

DOVGAL A. V., KOZLOV V. V., LEVCHENKO V. Y., 1980, Experimental investigation into the reaction of a boundary layer to external periodic disturbances, *Izv. Akad. Nauk SSSR, Mekh. Zhid. Gaza*, **4**, 155–159; (in Russian, English transl. 1981 in *Fluid Dyn.*, **15**, 4, 602–606).

GASTER M., GRANT I., 1975, An experimental investigation of the formation and development of a wave packet in a laminar boundary layer, *Proc. Roy. Soc. Lond. Ser. A*, **347**, 253–269.

GOLDSTEIN M. E., LEIB S. J., COWLEY, S. J., 1992, Distortion of a flat-plate boundary layer by free-stream vorticity normal to the plate, *J. Fluid Mech.*, **237**, 231–260.

GREK H. R., DEY J., KOZLOV V. V., RAMAZANOV M. P., TUCHTO O. N., 1991a, Experimental analysis of the process of the formation of turbulence in the boundary layer at higher degree of turbulence of windstream, Technical Report 91-FM-2, Indian Inst. Science, Bangalore, 560012, India.

GREK H. R., KOZLOV V. V., RAMAZANOV M. P., 1985, Three types of disturbances from the point source in the boundary layer, In *Laminar-Turbulent Transition*, KOZLOV V. V. Ed., Springer-Verlag, 267–272.

GREK H. R., KOZLOV V. V., RAMAZANOV M. P., 1991b, Laminar-turbulent transition at a high free stream turbulence level, *Siberian Phys.-Tech. J.*, **6**, 106–138, (in Russian).

GULYAEV A. N., KOZLOV V. E., KUZNETSOV V. R., MINEEV B. I., SEKUNDOV A. N., 1989, Interaction of a laminar boundary layer with external turbulence, *Izv. Akad. Nauk SSSR, Mekh. Zhid. Gaza*, **5**, 55–65; (in Russian, English transl. 1990 in *Fluid Dyn.*, **24**, 5, 700–710).

HENNINGSON D. S., 1995, Bypass transition and linear growth mechanisms, In *Advances in Turbulence V*, BENZI R. Ed., Kluwer, 190–204.

HENNINGSON D. S., ALFREDSSON P. H., 1987, The wave structure of turbulent spots in plane Poiseuille flow, *J. Fluid Mech.*, **178**, 405–421.

HERBERT T., LIN N., 1993, Studies of boundary-layer receptivity with Parabolized Stability Equations, AIAA Paper 93-3053.

KACHANOV Y. S., KOZLOV V. V., LEVCHENKO V. Y., 1978, Occurence of Tollmien-Schlichting waves in the boundary layer under the effect of external perturbations, *Izv. Akad. Nauk SSSR, Mekh. Zhid. Gaza*, **5**, 85–94, (in Russian, English transl. 1979 in *Fluid Dyn.*, **13**, 4, 704–711).

KENDALL J. M., 1985, Experimental study of disturbances produced in a pre-transitional laminar boundary layer by weak freestream turbulence, AIAA Paper 85-1695.

KENDALL J. M., 1990, Boundary layer receptivity to freestream turbulence, *AIAA Paper 90-1504*.

KENDALL J. M., 1991, Studies on laminar boundary-layer receptivity to freestream turbulence near a leading edge, In *Boundary Layer Stability and Transition to Turbulence*, REDA D. C., REED H. L., KOBAYASHI R. Eds., volume 114, 23–30.

KENDALL J. M., 1993, Boundary layer receptivity to weak freestream turbulence, Notes on figures presented at End-Stage Transition Workshop, August 15, 1993.

KLEBANOFF P. S., 1971, Effect of free-stream turbulence on a laminar boundary layer, *Bull. Am. Phys. Soc.*, **10**, 1323.

KLINGMANN B. G. B., BOIKO A. V., WESTIN K. J. A., KOZLOV, V. V., ALFREDSSON P. H., 1993, Experiments on the stability of Tollmien-Schlichting waves, *Eur. J. Mech., B/Fluids*, **12**, 493–514.

KOZLOV V. V., RYZHOV O. S., 1990, Receptivity of boundary layers: asymptotic theory and experiment, *Proc. Roy. Soc. Lond. Ser. A*, **429**, 341–373.

LANDAHL M. T., 1977, Dynamics of boundary layer turbulence and the mechanism of drag reduction, *Phys. Fluids*, **20** (10, Part II), 55–63.

LANDAHL M. T., 1980, A note on an algebraic instability of inviscid parallel shear flows, *J. Fluid Mech.*, **98**, 243–251.

LUCHINI P., 1996, Reynolds-number-independent instability of the boundary layer over a flat surface, *J. Fluid Mech.*, **327**, 101–115.

MORKOVIN M. V., RESHOTKO E., 1990, Dialogue on progress and issues in stability and transition research, In *Laminar-Turbulent Transition*, ARNAL D., MICHEL R. Eds., Springer-Verlag, 3–29.

NISHIOKA M., MORKOVIN M. V., 1986, Boundary-layer receptivity to unsteady pressure gradients: experiments and overview, *J. Fluid Mech.*, **171**, 219–261.

WATMUFF J. H., 1997, Detrimental Effects of almost immeasurably small free-stream nonuniformities generated by the wind tunnel screens, *AIAA Paper 97-0228.*

WESTIN K. J. A., BOIKO A. V., KLINGMANN B. G. B., KOZLOV V. V., ALFREDSSON P. H., 1994, Experiments in a boundary layer subjected to free-stream turbulence. Part I. Boundary layer structure and receptivity, *J. Fluid Mech.*, **281**, 193–218.

WYGNANSKI I., SOKOLOV M., FRIEDMAN D., 1975, On transition in a pipe. Part 2. The equilibrium puff, *J. Fluid Mech.*, **69**, 283–304.

(Manuscript received September 9, 1997,
Revised February 12, 1998;accepted March 12, 1998.)